

STUDY OF INDUCTION GENERATOR ISOLATED MODE

Makhlouf Laakam^{1,2}, Mehdi Dhaoui^{1,3}, Lassaâd Sbita^{1,3}

¹Research unit of Photovoltaic, Wind and Geothermal Systems

²Higher Institute of Technological Studies of Djerba

³National Engineering School of Gabes (ENIG)-Zrig 6029 Gabes, Tunisia.

ABSTRACT:

Wind energy schemes have the potential to substantially reduce the consumption of fossil fuels used in the production of electric energy. The self-excited induction generator has found renewed interest as a low maintenance wind generator for standalone and grid integrated applications. The aims of this paper are: the modelling and simulation of induction generator used in converting wind. First, we will start with turbine modelling. Second, we will deal with the two-phase modelling GAS cage while taking into account the saturation of the magnetic circuit. Then, concerning the simulation calculations, MATLAB®-SIMULINK® package is used to analyse the self-excited induction generator. Finally, the obtained practical results are presented, illustrating the limitations of the system.

KEY WORDS:

Induction generator, wind energy, self-excitation, practical results.

1. INTRODUCTION

The importance of wind energy as a clean, renewable energy source cannot be overstated; its ability to produce electric energy for standalone, micro-grid, and utility grid integrated applications has been repeatedly demonstrated. The role of the self-excited induction generator (SEIG) in these applications has grown as a result of its robust caged rotor construction, its low capital and maintenance costs, the absence of slip rings and brushes, inherent overload protection and its ability to produce energy over a wide range of wind speeds [1]-[3]. The asynchronous three-phase squirrel cage is used particularly in decentralized production of electricity as wind generator. In case the machine is connected to a power grid, it does not need an additional artificial excitation, if the network can provide the necessary reactive power. However, when operated in isolated mode, it is necessary to connect a capacitor bank across the asynchronous generator to eventually ensure self-excitation. This capacitor bank, in conjunction with the rest of magnetization (the residual) of the machine allows the latter to boot.

The objective of this paper is the modelling and studying of GAS cage used in converting wind. First, we will start with turbine modelling. Second, we will begin with the two-phase modelling GAS cage while taking into account the saturation of the magnetic circuit. Second, concerning the simulation calculations, MATLAB®-SIMULINK® package is used to analyse the self-excited induction generator. Finally, the obtained practical results are presented, illustrating the limitations of the system.

2. TURBINE MODELLING

The amount of power capacity produced by a wind turbine P_t is dependent on the power coefficient C_p . It is given by:

$$P_t = \frac{1}{2} \cdot C_p \cdot \rho \cdot \pi \cdot R^2 \cdot V^3 \quad (1)$$

Where ρ is the air density, R is the blade length and V the wind velocity. The turbine torque is the ratio of

the output power to the shaft speed Ω_t , $T_t = \frac{P_t}{\Omega_t}$.

The turbine is normally coupled to the generator shaft through a gear box whose gear ratio G is chosen so as to maintain the generator shaft speed within a desired speed range. Neglecting the transmission losses, the torque and shaft speed of the wind turbine, referred to the generator side of the gearbox, are given by:

$$T_{mec} = \frac{T_t}{G} \quad \text{and} \quad \Omega_{mec} = G \cdot \Omega_t \quad (2)$$

Respectively where T_{mec} is the driving torque of the generator and Ω_{mec} is the generator shaft speed.

A wind turbine can only generate a certain percentage of power associated with the wind. This percentage is represented by C_p which is the function of the wind speed, the turbine speed and the pitch angle of specific wind turbine blades [4].

Although this equation seems simple, C_p is dependent on the ratio λ between the turbine angular velocity Ω_t and the wind speed V . This ratio, called the tip speed ratio:

$$\lambda = \frac{R}{V} \cdot \Omega_t \quad (3)$$

A typical relationship between λ and C_p is shown in Figure 1. It is clear from this figure that there is a value of λ for which C_p is maximized, maximizing thus the power for a given wind speed. As depicted in Figure 2, the peak power for each wind speed occurs at the point where C_p is maximized. To maximize the generated power, it is therefore desirable for the generator to have a power characteristic that will follow the maximum C_{pmax} line.

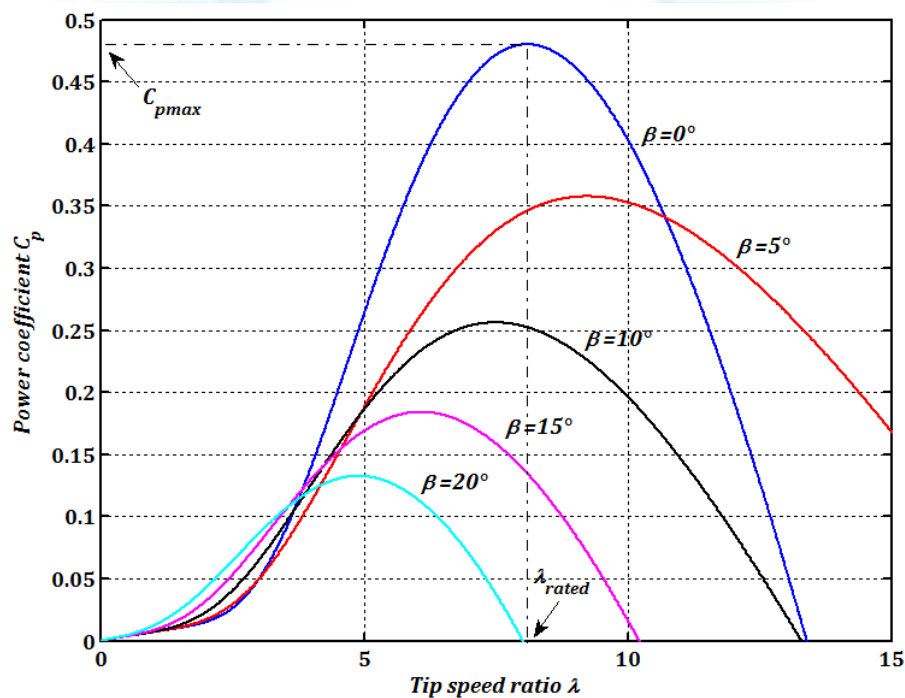


Figure 1. Power coefficient for the wind turbine model

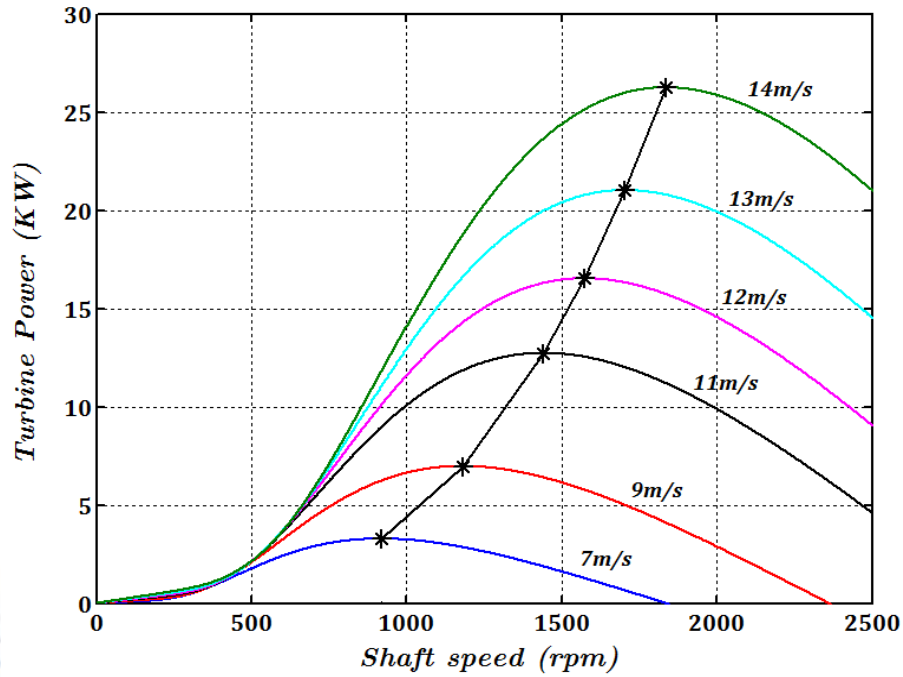


Figure 2. Power-Speed characteristics of the wind turbine

The action of the speed corrector must achieve two tasks:

- It must control mechanical speed Ω_{mec} with its reference $\Omega_{mec-ref}$.
- It must attenuate the action of the wind torque which constitutes an input disturbance.

The simplified representation in the form of diagram blocks is given in Figure 3.

Various technologies of correctors can be considered for the rotor speed control [5], [6].

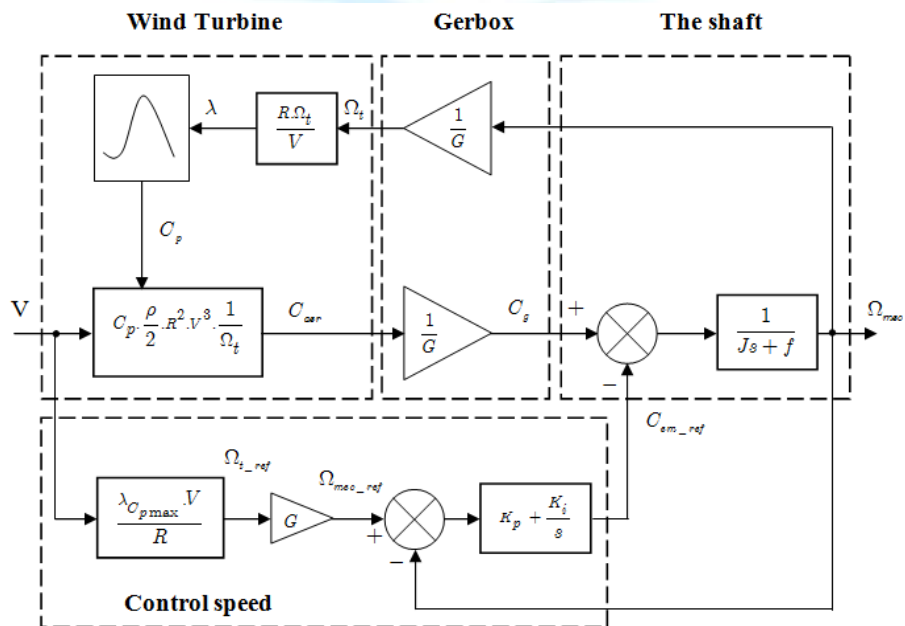


Figure 3. Device control with control speed

3. THE MODEL OF THE ASYNCHRONOUS MACHINE

The mathematical model used in this case is known as Park. Indeed, the magnetic field produced by the three-stator coils supplied with a three-phase electric system (V_a, V_b, V_c) can be obtained by means of two coils with perpendicular axes and are fed by a two-phase equivalent system (V_{sd}, V_{sq}). By means of the transformation of Park, we obtain the equations of this bi-phase machine [7].

Electrical equations become:

The stator:

$$\begin{cases} v_{ds} = R_s \cdot i_{ds} - \phi_{qs} \left(\frac{d\theta_s}{dt} \right) + \frac{d\phi_{ds}}{dt} \\ v_{qs} = R_s \cdot i_{qs} - \phi_{ds} \left(\frac{d\theta_s}{dt} \right) + \frac{d\phi_{qs}}{dt} \end{cases} \quad (4)$$

The rotor:

$$\begin{cases} v_{dr} = R_r \cdot i_{dr} - \phi_{qr} \left(\frac{d\theta_r}{dt} \right) + \frac{d\phi_{dr}}{dt} \\ v_{qr} = R_r \cdot i_{qr} - \phi_{dr} \left(\frac{d\theta_r}{dt} \right) + \frac{d\phi_{qr}}{dt} \end{cases} \quad (5)$$

4. SELF-EXCITATION

The self-excitation of the generator starts with the residual flux and the rotor rotation, creating a low voltage across the cage induction generator; this will increase voltage across the capacitor. This process will be repeated till the moment when the voltage returned by the capacitor is equal to the nominal voltage of the generator (operating point) [1]-[3]. When the machine is driven over the synchronous speed, the machine operates as an alternative generator. In the autonomous mode, the stator must be necessarily connected to the capacitors as it will strengthen the remanent magnetic field which is necessary for magnetizing the machine and hence generating the rotor's current to create a reactive current that will enhance the preceding remanent field,. This reaction cycle will allow the machine to reach the operating point located in the saturated zone. When the machine is not saturated, the magnetization characteristic $\phi(I_m)$ is a line of slope approximately equal to the mutual L_m . To work in the saturated regime, it is necessary that the magnetic inductance $L_m(I_m) \neq \text{constant}$.

5. THE ASYNCHRONOUS GENERATOR WITHOUT LOAD

The equivalent model of the asynchronous generator in the reference (d, q) leads to the following equations: where L_s and L_r are the inductors of the stator and rotor phase, L_m is the magnetizing inductor, R_r and R_s are rotor and stator resistances respectively [1]-[3] and [8].

$$\begin{bmatrix} \phi_{ds} \\ \phi_{dr} \end{bmatrix} = \begin{bmatrix} L_s & L_m \\ L_m & L_r \end{bmatrix} \cdot \begin{bmatrix} I_{ds} \\ I_{dr} \end{bmatrix} \quad (6)$$

And

$$\begin{bmatrix} \phi_{qs} \\ \phi_{qr} \end{bmatrix} = \begin{bmatrix} L_s & L_m \\ L_m & L_r \end{bmatrix} \cdot \begin{bmatrix} I_{qs} \\ I_{qr} \end{bmatrix} \quad (7)$$

Choosing a repository (d, q) stator related $\omega_s = 0$ and $\omega = -\omega_r$, the system becomes:

$$\begin{cases} L_s \frac{dI_{ds}}{dt} + L_m \frac{dI_{dr}}{dt} = -R_s \cdot I_{ds} - V_{ds} \\ L_s \frac{dI_{qs}}{dt} + L_m \frac{dI_{qr}}{dt} = -R_s \cdot I_{qs} - V_{qs} \\ L_m \frac{dI_{ds}}{dt} + L_r \frac{dI_{dr}}{dt} = -\omega \cdot L_m I_{qs} - R_r I_{dr} - \omega \cdot L_r I_{qr} \\ L_m \frac{dI_{qs}}{dt} + L_r \frac{dI_{qr}}{dt} = \omega \cdot L_m I_{ds} - R_r I_{qr} + \omega \cdot L_r I_{dr} \end{cases} \quad (8)$$

Applying Ohm's law to each phase, we obtain:

$$\begin{cases} C \cdot \frac{dv_{ds}}{dt} = i_{ds} \\ C \cdot \frac{dv_{qs}}{dt} = i_{qs} \end{cases} \quad (9)$$

Writing in matrix form of this system is:

$$\begin{bmatrix} L_s & 0 & L_m & 0 & 0 & 0 \\ 0 & L_s & 0 & L_m & 0 & 0 \\ L_m & 0 & L_r & 0 & 0 & 0 \\ 0 & L_m & 0 & L_r & 0 & 0 \\ 0 & 0 & 0 & 0 & 1 & 0 \\ 0 & 0 & 0 & 0 & 0 & 1 \end{bmatrix} \begin{bmatrix} \frac{dI_{ds}}{dt} \\ \frac{dI_{qs}}{dt} \\ \frac{dI_{dr}}{dt} \\ \frac{dI_{qr}}{dt} \\ \frac{dV_{ds}}{dt} \\ \frac{dV_{qs}}{dt} \end{bmatrix} = \begin{bmatrix} R_s & 0 & 0 & 0 & -1 & 0 \\ 0 & R_s & 0 & 0 & 0 & -1 \\ 0 & -X_m & -R_r & -X_r & 0 & 0 \\ X_m & 0 & X_r & -R_r & 0 & 0 \\ \frac{1}{C} & 0 & 0 & 0 & 0 & 0 \\ 0 & \frac{1}{C} & 0 & 0 & 0 & 0 \end{bmatrix} \cdot \begin{bmatrix} I_{ds} \\ I_{qs} \\ I_{dr} \\ I_{qr} \\ V_{ds} \\ V_{qs} \end{bmatrix} \quad (10)$$

With

$$X_m = \omega \cdot L_m \text{ and } X_r = \omega \cdot L_r$$

We designed the asynchronous form of state or a system of six equations where we chose the state vector as follows:

$$[X] = \begin{bmatrix} I_{ds} \\ I_{qs} \\ I_{dr} \\ I_{qr} \\ V_{ds} \\ V_{qs} \end{bmatrix}$$

$$[L] = \begin{bmatrix} L_s & 0 & L_m & 0 & 0 & 0 \\ 0 & L_s & 0 & L_m & 0 & 0 \\ L_m & 0 & L_r & 0 & 0 & 0 \\ 0 & L_m & 0 & L_r & 0 & 0 \\ 0 & 0 & 0 & 0 & 1 & 0 \\ 0 & 0 & 0 & 0 & 0 & 1 \end{bmatrix}$$

$$[B] = \begin{bmatrix} R_s & 0 & 0 & 0 & -1 & 0 \\ 0 & R_s & 0 & 0 & 0 & -1 \\ 0 & -X_m & -R_r & -X_r & 0 & 0 \\ X_m & 0 & X_r & -R_r & 0 & 0 \\ \frac{1}{C} & 0 & 0 & 0 & 0 & 0 \\ 0 & \frac{1}{C} & 0 & 0 & 0 & 0 \end{bmatrix}$$

This model is written by:

$$[\dot{X}] = [A][B][X]$$

Where:

$$[A] = [L]^{-1} \text{ and } [\dot{X}] = \frac{d}{dt}[X] = S.X$$

[L]: is the matrix of inductances

S: Laplace operator.

6. SIMULATION RESULTS AND DISCUSSION

The interaction of the two phenomena, remanence magnetization and capacitors cause the booting of the machine to the point of continuous operation. The observation of these curves shows easily that residual values and capacitors can change the location of the operating point on the magnetization characteristic. The self-excitation is simulated in case the machine is driven at 1500 rpm without load and magnetized by a self-excitation capacity of 75 μ F.

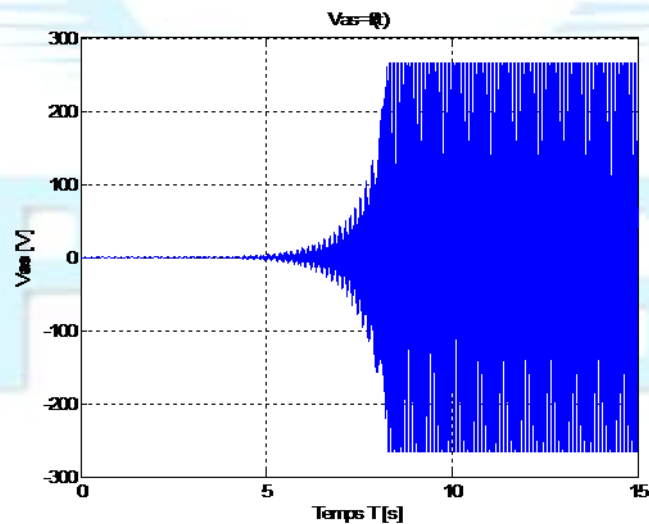


Figure 4. Simulated self-excitation at 1500rpm and 75 μ F: generated voltage.

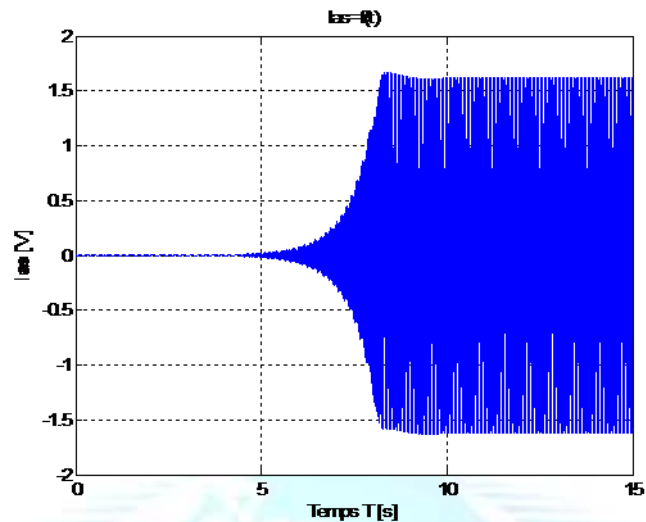


Figure 5. Simulated self-excitation at 1500rpm and 75µF: generated current

These figures show the curves of the stator voltage and current from the transient to the permanent mode. We note that the voltage and current of the stator behave exponentially in the area of unsaturation $t = [0, 8]$, then they converge to a fixed value in the saturated zone out = $[8, 15]$. The boot up time is about 8s. The amplitudes of the stator currents and voltages obtained are equal to 270V and 1.7 A, with a frequency of 50Hz.

6.1 Influence of saturation

According to (Figure 6), we see that the magnetizing inductance varies non-linearly according to the law

$$L_m = f(v) ;$$

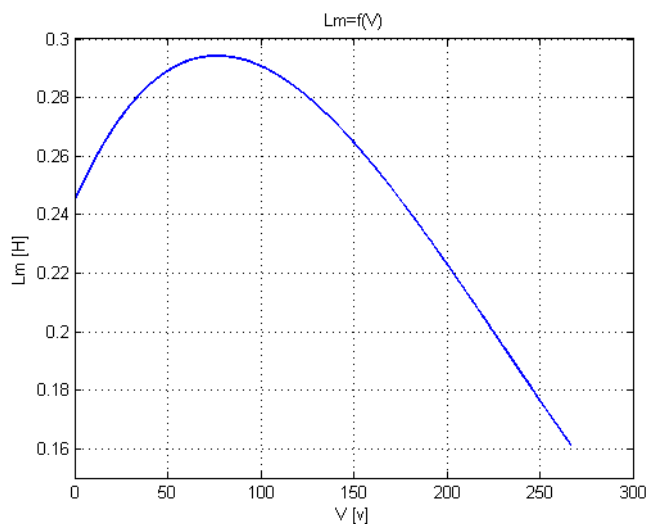


Figure.6. Variation of magnetizing inductance with phase voltage.

In a non-saturated regime the magnetizing inductance is regarded as constant, the magnetization characteristic does not bend when saturation. The self-excitation is possible but the stator voltage then increases to an infinite theory value.

6.2 Influence of the remanent field

The remanent field is the residue of magnetization of the machine, which allows the latter to begin. The rest of this increase leads to reduce the boot time, the (Figure 7) and (Figure 8) show the terminal voltage obtained for two values of the remanent field x_1 and x_2 with $x_1 > x_2$ and $n = 1500$ rpm, $C = 75\mu\text{F}$.

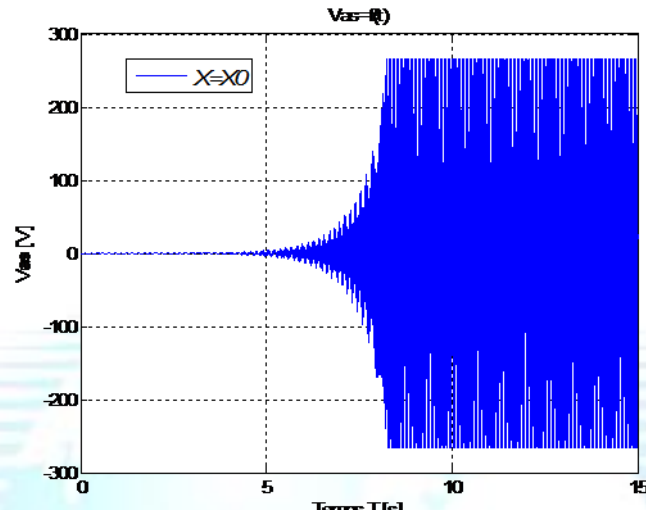


Figure 7. The terminal voltage built up at $X=X_0$.

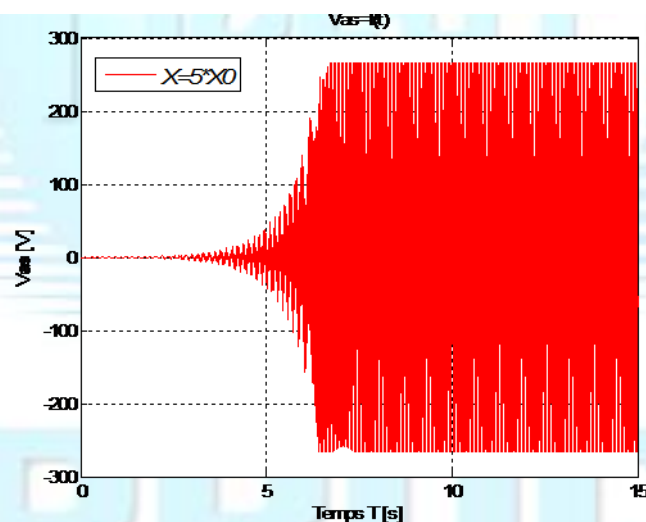


Figure 8. The terminal voltage built up at $X=5X_0$.

The results obtained with the two values of X with $X_1 = X_0$ and $X_2 = 5X_0$ with (X_0 represents the remanent field in $i_{ds} = i_{qs} = i_{dr} = 0.01\text{A}$).

6.3 Influence of Speed

Speed has a direct influence on the voltage for the same magnetizing current. A passage from 1500 rpm to 1200 rpm, which represents a 20% variation causes a 17.6% variation of current which is illustrated in (Figure 9) and (Figure 10).

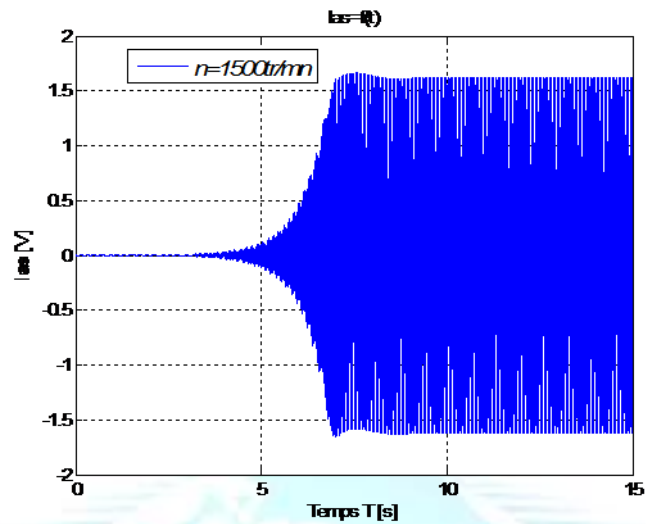


Figure 9. Generated current at 1500rpm.

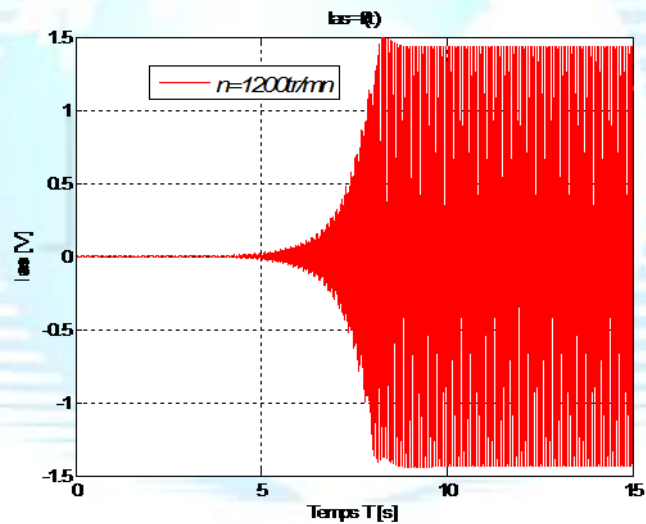


Figure 10. Generated current at 1200rpm.

The frequency is linearly related to the velocity in the equation: $f_s = \frac{n \cdot p}{60}$ ($g \approx 0$). (11)

7. EXPERIMENT RESULTS AND DISCUSSION

For the practical implementation we used an experimental stand composed of a DC motor which has a separate excitation and three-phase induction machine, a tachometer to measure the speed, a shunt to view the current supplied by the generator, a differential probe voltage of 1/1000 to see the line voltage, a digital oscilloscope, load banks capacitive and resistive and optionally measuring devices.



Figure 11. Experimental stand.

The machine is being without load when driven by the wind turbine, we also notice the appearance of a voltage across its terminals if there is a remanent field. The visualization using an oscilloscope of the voltage generated at the stator of the machine and the network decoupled without load with any excitation is shown in Figure 12. This voltage is relatively low due to the remanence and the fact that the rotor is rotated.

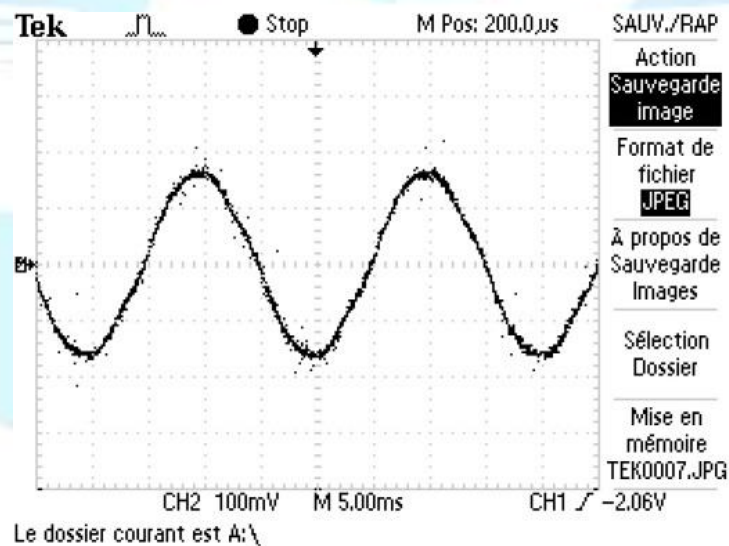


Figure 12. Measured voltage with no excitation.

It should therefore lead to a usable value by increasing the magnetic flux in the machine by connecting a capacitor. It has a bench 2kvars. The asynchronous machine is driven at a speed of 1500 rpm. It puts operating capacitors gradually until there is a stable value RMS voltage between phases.

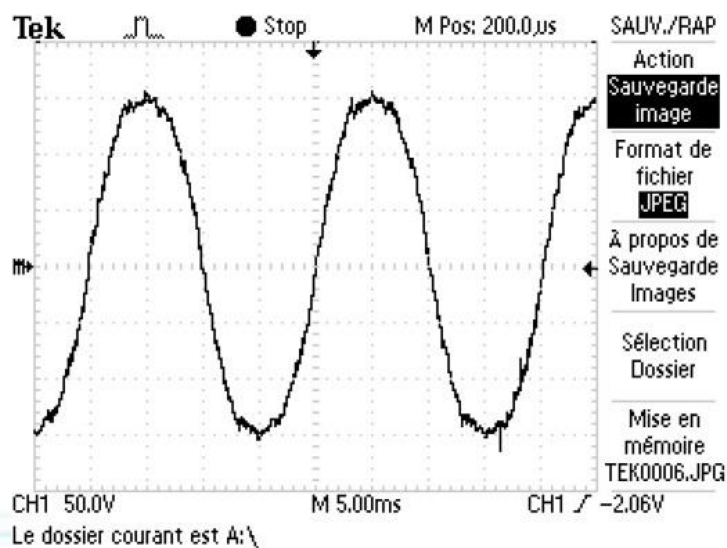


Figure 13. Measured voltage between phases.

The following figure shows the image of speed after a tachogenerator.

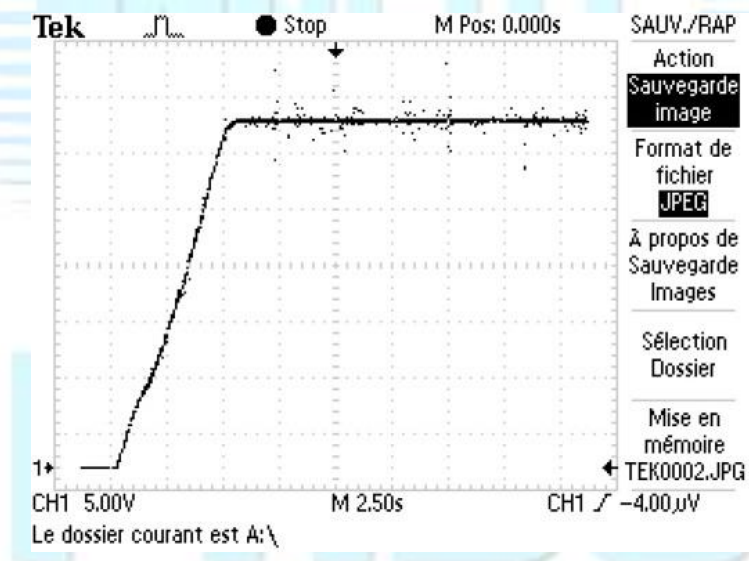


Figure 14. Measured speed at 60 µF.

This waveform is used to highlight the 90 ° phase shift of the current before the voltage.

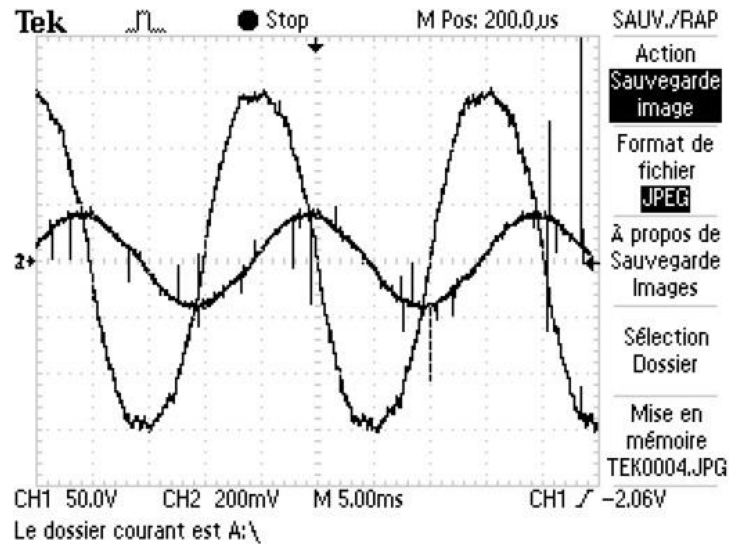


Figure 15. Steady-state voltage and current waveforms from oscilloscope for the isolated IG operated at 50Hz.

By analogy with the synchronous machine, we can say that the ability plays a similar role of the current excitation which is therefore the variable of the terminal voltage of the generator.

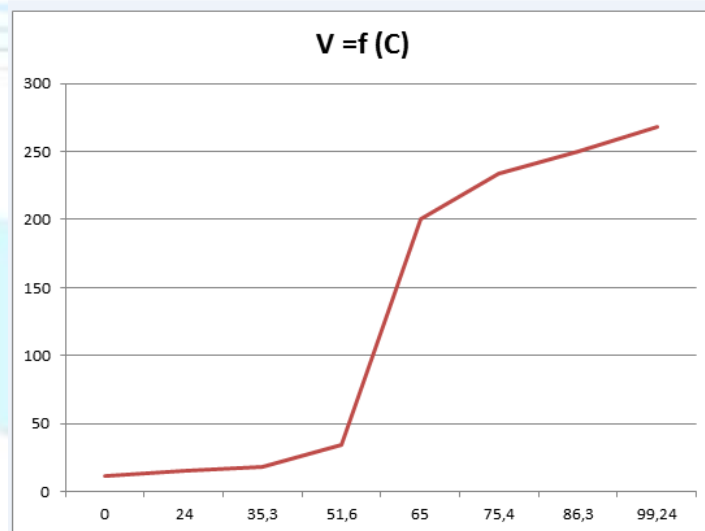


Figure16. Measured voltage versus the excitation.

The curve is not linear and therefore it shows the difficulty of controlling the voltage output. In fact there is no simple relationship between the excitation and voltage output.

8. CONCLUSION

This paper discusses the operation of an induction machine under standalone generating mode. A laboratory test is performed where the induction machine is controlled as a self-excited induction generator. The dynamic analysis of a self-excited induction generator is done and the effects of rotor speed, the remanent field and excitation capacitance are observed. From the simulation and experimentation, it is confirmed that as the capacitance increases at a particular speed, voltage builds up faster and the magnitude of voltage increases due to the availability of more VAR. In stand-alone mode the two quantities power and voltage are related, and therefore a change in velocity causes a variation in power and voltage. The excitation variation causes a variation in the voltage output and consequently power. If a receiver absorbs a fixed power it must then act on the excitation to control voltage. Note that the risks arising from the use of a capacitor bank to compensate an induction generator are high. If the batteries are connected, voltage output at the terminals of the windings during the stop phase is high. Above all, it is not enough to disconnect the motor from its source to be protected when responding during the stop phase because the machine is self-excited by the capacitor bank.

REFERENCES

- [1] D. Seyoum, C. Grantham and F. RAHMAN, (2003) "Analysis of an isolated self-excited induction generator driven by a variable speed", the University of New South Wales March.
- [2] Debta, Birendra Kumar and Mohanty, K.B, (2010) "Analysis on the effect of dynamic mutual inductance in voltage buildup of a stand-alone brushless asynchronous generator", Procc.of National Power Electronics Conference, June.
- [3] Ali Nesba, Rachid Ibtouen, Toohami, (2006) " Dynamic performance of self-excited induction generator feeding different static loads, Serbian Journal of Electrical Engineering", vol. 3, no.1, June, pp.63-76.
- [4] N. Aouani, F. Bacha, R. Dhifaoui, (2009) "Control Strategy of a Variable Speed Wind Energy Conversion System Based on a Doubly Feed Induction Generator ", IREACO, Vol.2, no.2, March.
- [5] M. Dhaoui, (2011) "Optimisation du fonctionnement de l'actionneur à induction par logique floue, les réseaux de neurones et les algorithmes génétiques", Doctorat Thesis ENIG, University of Gabes, Tunisia.
- [6] K.B. Mohanty, (2008) "Study of Wind Turbine Driven DFIG Using AC/DC/AC Converter", PhD thesis, National Institute of Technology Rourkela,.
- [7] Venkatesa Perumal, B. and Chatterjee, Jayanta K.,(2008) "Voltage and Frequency Control of a Stand Alone Brushless Wind Electric Generation Using Generalized Impedance Controller" , IEEE Trans. on Energy Conversion, vol. 23, no.2, June, pp.632-641.
- [8] M. Laakam, H. Ammi , M. N. Abdelkarim et L. Sbita, (2007) " Fuzzy Logic Application to the Motor Induction Control", Fourth International Multi-Conference on Systems, Signals & Devices March 19-22, Hammamet, Tunisia.

Authors

Lassaâd Sbita obtained the doctorate thesis in July 1997 in Electrical engineering from ESSTT of Tunis, Tunisia. He works as an associate Professor at the electrical-automatic genius department of the National Engineering School of Gabes, Tunisia. His fields of interest include power electronics, machine drives, automatic control, modelling, observation and identification.



Mehdi Dhaoui obtained the doctorate thesis in May 2011 in Electrical engineering from ENIG, Tunisia. He works as an associate Professor at the electrical-automatic genius department of the National Engineering School of Gabes, Tunisia. His fields of interest include power electronics, machine drives, automatic control, modeling, identification and optimization. He uses the intelligent technical Genetic algorithm, Fuzzy logic and Neuronal Network.



Laakam Makhoul obtained the master degree of automatic and industrial computer sciences in May 2003 from the National School of Engineering in Sfax ENIS, Tunisia. Currently, he works as a Technologue Teacher, at the Higher institute of Technological Studies of Djerba, Tunisia. His fields of interest include power electronics, machine drives, automatic control and Fuzzy logic.

